ELSEVIER

Journal of Magnetism and Magnetic Materials 226–230 (2001) 1370–1376

Journal of magnetism and magnetic materials

www.elsevier.com/locate/jmmm

New permanent magnets

K.-H. Müller*, G. Krabbes, J. Fink, S. Gruß, A. Kirchner, G. Fuchs, L. Schultz

Institute of Solid State and Materials Research, IFW Dresden, P.O. Box 270016, D-01171 Dresden, Germany

Abstract

Permanent magnets play an important role and are widely spread in daily-life applications. Due to their very low costs, large availability of the row materials and their high chemical stability, hard ferrites are still dominant in the permanent magnet market although their relatively poor magnetic properties are a distinct disadvantage. Today's high-performance magnets are mostly made from $Nd_2Fe_{14}B$. The aim of research is to combine the large spontaneous magnetization of 3d metals with strong anisotropy fields known from rare-earth transition-metal compounds and, at the same time, to maintain a high value of the Curie temperature. However, the number of iron-rich rare-earth intermetallics is very limited and, consequently, not much success can be noted in this field for the last 10 years. One alternative concept is to use magnetic fields trapped in type II superconductors where much higher fields can be achieved compared to conventional rare-earth magnets. Very recently, we obtained a trapped field as high as 14.4 T in a melt-textured YBCO bulk sample of a few centimeters in diameter. This is the highest value ever achieved in a bulk superconductor. The trapped field of a superconductor is not governed by the Laplace equation and, therefore, levitation works without any additional (active) stabilization. The disadvantage of these magnets is their low working temperature (of liquid nitrogen and below).

Keywords: Permanent magnets; Magnetic levitation; Superconducting permanent magnets; Superconducting bearings

1. Introduction

Permanent magnets have been used by man for thousands of years. Today they play an important role and are widely spread in daily-life applications [1]. Up to now permanent magnets have always been produced from ferromagnetic alloys or compounds and, in particular in the last century, much progress has been made in improving permanent-magnet properties. However, it is generally accepted that the saturation magnetization of future ferromagnetic permanent magnets will never exceed the known values of the spontaneous magnetization of 3d transition metal alloys (see Section 2). Therefore, beyond the search for novel compounds as candidates for future magnets completely new approaches have also to be considered. One alternative concept is to use magnetic fields trapped in type II superconductors [2]. As will be shown in Section 3 a trapped field as high as 14.4 T has been achieved in a melt-textured YBCO bulk sample of a few centimeters in diameter. Hence, much higher fields can be realized using such superconducting permanent magnets compared to conventional rare-earth magnets. A special feature of the type II superconductors is that their trapped fields are not governed by the Laplace equation (as in the case of ferromagnetic permanent magnets) and, therefore, levitation works without any additional (active) stabilization. Depending on the field configuration being present during cooling of the superconductor, the levitated body (e.g. a ferromagnetic permanent magnet) may be fixed on a single position in space or may have one degree of freedom, as a train on the rails, or two degrees of freedom on a plane. A much discussed application of such levitation is the construction of bearings, for rotating machines, with non-contacting surfaces and without an active feedback system [2]. The disadvantage of these magnets is their low working temperature (of liquid nitrogen and below).

* Corresponding author. Fax: +49-351-4659-537.
E-mail address: khm@ifw-dresden.de (K.-H. Müller).

0304-8853/01/$ - see front matter
PII: S0304-8853(00)00913-6

2. Rare-earth permanent magnets

If a ferromagnetic compound has a large spontaneous magnetization J_s combined with a high Curie temperature T_c and a strong anisotropy field H_A it is considered to be a good candidate for permanent magnet materials. However, a magnetized permanent magnet is in a thermodynamically metastable state whose stability is controlled by non-equilibrium processes such as nucleation of reverse domains, depinning of domain walls, etc. These processes are very sensitive to the microstructure of the material. Therefore, permanent magnets are characterized by so-called extrinsic magnetic properties as the coercive field ${}_JH_c$, the remanence induction B_r, the storable energy density $(BH)_{max}$ and the maximum working temperature T_m. The extrinsic properties of a material depend on J_s, T_c, H_A but also on details of the chemical and topological microstructure. In the case of Alnico and Fe–Cr–Co magnets the microstructure is even responsible for the magnetic anisotropy (shape anisotropy) whereas in the majority of permanent magnets the magnetic hardness is based on H_A resulting from magnetocrystalline anisotropy in non-cubic phases, as e.g. in hard ferrites, (Co, Fe)–Pt alloys, Mn–Al magnets and rare-earth transition-metal compounds [1]. The highest value of the "energy product" $(BH)_{max}$, which is considered to be the most important extrinsic property, has so far been achieved for $Nd_2Fe_{14}B$-based magnets (Fig. 1). This value is close to the upper limit $J_s^2/4\mu_0$ of this compound. Therefore, $(BH)_{max}$ can only be remarkably increased if novel compounds will be found which exhibit larger J_s, connected with sufficient large H_A [1]. The intrinsic properties of various Fe-rich rare-earth transition-metal compounds could be considerably improved by interstitial modification (with C or N) or substitutional modification [1,3]. Even new phases have been found as e.g. the tetragonal compound $SmFe_7$ [4]. But not much success in the intrinsic magnetic properties, compared to that of $Nd_2Fe_{14}B$, can be noted in the last decade. Due to their very low costs, wide availability of the raw materials and their high chemical stability, hard ferrites are still dominant (with about 55%) in the permanent magnet market (see Fig. 2) although their low $(BH)_{max}$ is a distinct disadvantage. Now the market of Nd–Fe–B magnets is expanding at the expense of hard ferrites [5,6]. A weak point of the Nd–Fe–B magnets is their relatively low resistance against corrosion which, however, could remarkably be improved by modifying the intergranular phase with Co, Cu, Al, and Ga [7]. Success can also be noted in texturing of fine-grained Nd–Fe–B materials by hot deformation (see Fig. 3). A further interesting novel type of Nd–Fe–B magnets are the single-phase or multi-phase fine-grained materials showing remanence enhancement caused by exchange interaction [9]. Novel field sources called "magic rings" and "magic spheres" have been developed that exhibit considerably higher fields than the B_r of the used Nd–Fe–B material [10]. Sometimes new magnets have been developed because there is a strong need for the improvement of certain extrinsic properties and because modified preparation routes have been elaborated. As an example Sm–Co

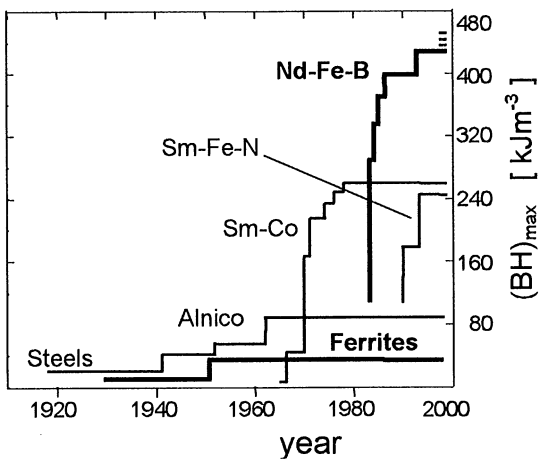

Fig. 1. Development, in the 20th century, of the achieved values of the energy density $(BH)_{max}$ of permanent magnet materials.

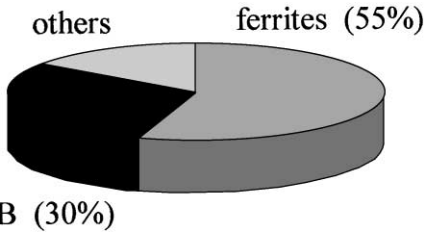

Fig. 2. Estimate of the worldwide market for permanent magnet materials.

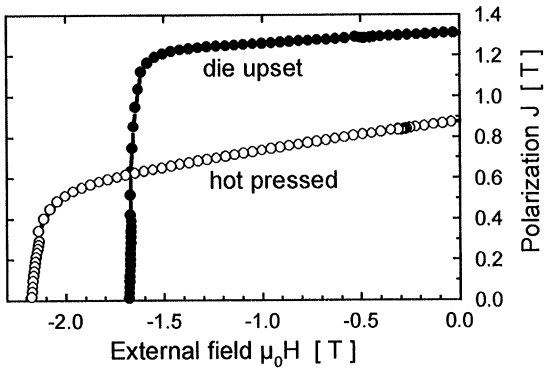

Fig. 3. Demagnetization curves of isotropic (hot pressed) and textured by hot deformation (die upset) commercial melt-spun Nd–Fe–B powder MQU-F [8].

magnets conventionally prepared by sintering can now be produced as fine-grained magnets by hydrogenation disproportionation desorption recombination (HDDR) under extreme conditions [11] i.e. under high hydrogen pressure [12] or by means of reactive milling [13]. Such materials can be used for higher temperature than Nd–Fe–B magnets because $SmCo_5$ and Sm_2Co_{17} have higher values of T_c than $Nd_2Fe_{14}B$ and the fine-grained Sm–Co materials are more stable than conventional Sm–Co magnets. Sintered Sm–Co magnets have also successfully been modified to be applicable for higher temperatures [14,15].

In conclusion, an increasing market and a steady improvement of commercial rare-earth transition-metal magnets can be observed. But no dramatic enlargement of $(BH)_{max}$ of ferromagnetic permanent magnets can be noted for the last decade or will be expected for the near future. The aim of research is to combine the large spontaneous magnetization of transition metals (as e.g. 2.43 T in $Fe_{65}Co_{35}$ — the highest value of J_s ever achieved) with the strong anisotropy fields known from rare-earth transition-metal compounds (e.g. 40 T in $SmCo_5$) and, at the same time, to maintain a high value of T_c.

3. Superconducting permanent magnets

Trapped fields in bulk type II superconductors are generated by supercurrents circulating macroscopically within the material. The main features of the field distribution are a maximum trapped field B_0 in the center of a well-textured superconducting area, usually called domain, and a field gradient toward the domain edge which is determined by the critical current density j_c of the supercurrents. Therefore, high trapped fields B_0 require a high critical current density and a large size of the current loops. Large single-domain $YBa_2Cu_3O_{7-x}$ (YBCO) material can be obtained by melt-texture processing, especially by using $SmBa_2Cu_3O_{7-x}$ (Sm-123) as a seed crystal. The main problem to obtain high critical current densities in melt-textured YBCO is to create a defined microstructure with defects as small as the coherence length of 1.8 nm. The pinning can be improved by irradiation techniques [16]. Using this method high critical current densities up to 85 kA/cm^2 and trapped fields up to 2.1 T measured on the top of a single YBCO disk were obtained at 77 K [17]. For comparison, the highest trapped fields achieved at 77 K for non-irradiated bulk YBCO are in the range slightly above 1 T [18,19].

Cracking of the bulk YBCO material was found to limit the trapped field at lower temperatures which is due to the tensile stress occurring during the magnetization process and exceeding the tensile strength of YBCO [20]. The relatively low tensile strength observed for bulk YBCO is caused by the presence of small cracks propagating when the applied tensile stress reaches the fracture toughness K_c. The tensile strength of YBCO containing additions of silver has been found to increase up to 30–40 MPa [21]. Even 70 MPa have been reported in the past [22]. In this section, the combined influence of Ag addition and a bandage made from a steel tube filled with epoxy on the trapped field of YBCO will be reported. Furthermore, the improved pinning properties of zinc-doped YBCO are presented and compared with results for $NdBa_2Cu_3O_{7-x}$ (Nd-123).

3.1. Experimental

Melt-textured YBCO bulk samples were prepared with varying content of zinc and silver admixtures using Sm-123 as seed crystal. Small amounts of zinc < 1 wt% were added in order to improve the pinning properties or an admixture as large as 10 wt% Ag was applied to enhance the mechanical strength of the material. Details of the sample preparation are reported elsewhere [23,24]. Large-domain monoliths up to 50 mm in diameter are obtained by the melt process. The a, b planes of the large grains are oriented parallel to the plane of the cylindrically shaped samples. The microstructure revealed small, homogeneously distributed Y-211 precipitates 200–1000 μm in size and, if Ag was added, supplementary inclusions of Ag droplets. The YBCO disks were characterized at 77 K by field mapping of the trapped field and by measuring the levitation forces. The distribution of the trapped field in the superconductor was scanned by means of a Hall sensor with a small active area of 0.2 mm^2. The temperature dependence of the maximum trapped field B_0 was investigated for a fixed position of a Hall sensor on the top of single YBCO samples as well as in the 1 mm gap between two disks. In order to compensate the magnetic tensile stresses being enhanced during the magnetizing procedure on the YBCO disks, they were placed into 2-mm-thick steel tubes. Stycast epoxy was filled in the small space between the YBCO disks and the steel tubes applying a vacuum impregnation technique. The steel tube produces a compressive stress on the YBCO disks after cooling down from 300 K to the measuring temperature. These measurements were performed in the variable temperature cryostat of a superconducting 18 T magnet. For magnetizing the bulk YBCO sample a magnetic field was applied at a temperature above T_c. After cooling the sample to the measuring temperature, the magnetic field was reduced to zero and B_0 was recorded by means of the Hall sensor. Alternatively the samples have also been magnetized by pulsed fields. The magnetization of small cylindrical samples prepared from the large YBCO disks was investigated in a vibrating sample magnetometer. Critical current densities were determined from magnetic hysteresis curves.

3.2. Improved pinning in zinc-doped YBCO and its effect on trapped fields

Typical field profiles of single-grain YBCO disks are shown in Fig. 4. The different shape of the field distribution in the undoped and the zinc-doped material reflects different field dependencies of the critical current density j_c which are shown in Fig. 5. The gradient of the field profile of the undoped YBCO disk decreases with increasing trapped field which is attributed to the monotonous decrease of j_c with increasing applied field at temperatures around 77 K. On the other hand, the field gradient of the zinc-doped YBCO disk remains almost constant to the maximum trapped field which is connected with the pronounced so called peak effect in the field dependence of the critical current density observed for zinc-doped YBCO. It is obvious that the peak effect is very advantageous for obtaining high trapped fields. We found at 77 K an improvement of the maximum trapped field B_0 from about 0.8 T for undoped YBCO disks up to 1.1 T for zinc-doped YBCO disks 25 mm in diameter. The characteristic maximum in the $j_c(B)$ dependence of zinc-doped YBCO was observed to increase with decreasing temperature in height and to shift to higher magnetic fields as can be seen in Fig. 5. At 75 K, the critical current density of the Zn-doped sample passes through a maximum at $B_m = 2$ T, which is shifted up to 5 T at 55 K. Compared with the undoped reference material, the Zn-doped YBCO has, at 75 K, enhanced j_c values in the field range of the maximum of the critical current density, whereas at 55 K a considerable improvement of j_c of the Zn-doped material is observed in the whole investigated field range $B < 8$ T, including zero-magnetic field. The peak effect in Nd-123 has been attributed to strong pinning caused by extended superconducting defects with reduced T_c [25]. A possible explanation for the peak effect in Zn-doped YBCO has been proposed recently [19]. It is well known that T_c of YBCO is strongly suppressed by Zn-doping [26]. The non-magnetic Zn impurities occupy the in-plane Cu sites. Whereas the doped holes in the standard CuO_2 plane compensate the copper spins, a doped hole in the neighborhood of a zinc impurity induces a local magnetic moment which may result in pair breaking of the superconducting carriers. The disturbed regions around the Zn impurities have an extension of about 1.5 nm as was found by NMR investigations [27]. Therefore, these regions have almost the optimum size for the pinning of flux lines which is given by the superconducting coherence length $\xi = 1.8$ nm for YBCO. Thus, the disturbed region around a Zn impurity can be considered as a superconducting precipitate with strongly reduced superconducting parameters. By applying a magnetic field these superconducting precipitates may be driven into the normal state resulting in improved pinning and the peak effect observed for small Zn concentrations.

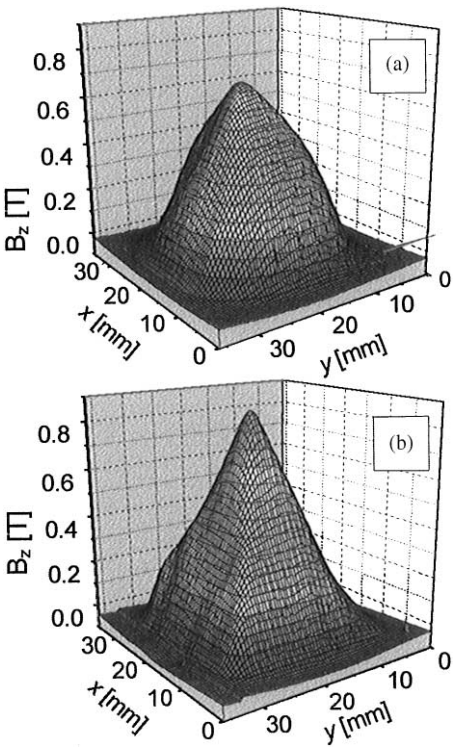

Fig. 4. Field profiles of the trapped field B_z measured at 77 K on the top of YBCO disks. (a) Undoped; (b) Zn-doped.

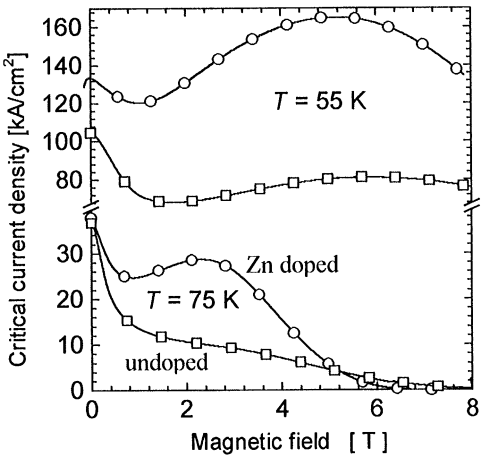

Fig. 5. Critical current density vs. applied magnetic field for undoped and Zn-doped YBCO measured at two different temperatures.

3.3. High trapped field and cracking

For all temperatures under investigation the Zn-doped YBCO disk has higher trapped fields than the non-doped

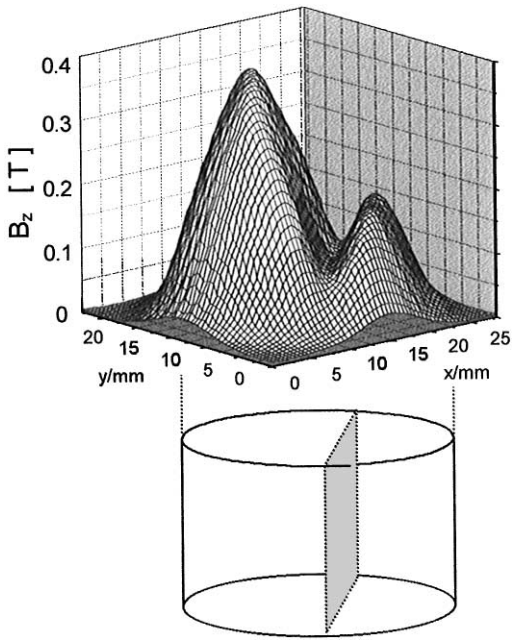

Fig. 6. Field profile of a YBCO disk after cracking. The corresponding two superconducting domains are shown schematically in the lower part of the figure.

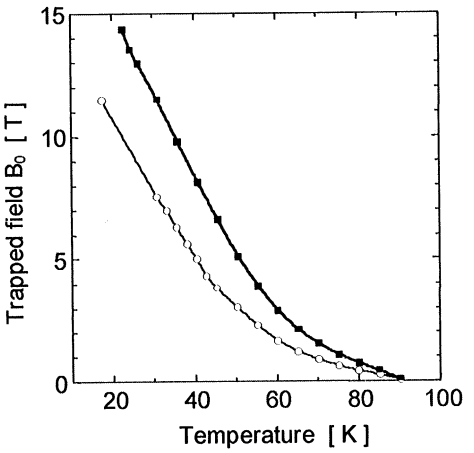

Fig. 7. Temperature dependence of the maximum trapped field B_0 for YBCO disks containing 10 wt% Ag. Open circles: single YBCO disk; solid squares: YBCO disk pair. In both cases, a bandage made of a steel tube filled with epoxy was used.

YBCO disk, which is due to the enhanced critical current density in the Zn-doped material. Without steel tube, cracking of the Zn-doped disk was observed at 57 K, limiting the maximum trapped field on a value of $B_0 = 4.4$ T at $T = 58$ K. By using a steel tube the trapped field of that disk was enhanced up to $B_0 = 9$ T at 43 K, before cracking occurred at 42 K. Cracking is indicated by a sudden decrease of the signal of the Hall sensor. A visual inspection of damaged samples shows the crack in some cases on the surface of the sample, but sometimes no crack is visible. Cracks within the disk can be investigated by field profile measurements at 77 K. The field profile of a damaged sample is shown in Fig. 6. The crack divides the sample into two superconducting domains. Currents can flow only within these domains, but not across the boundary between them. The distribution of the tensile stress within a bulk superconductor during the activation process was calculated by Ren et al. [20] for long cylindrical samples. Recently, this model has been extended to arbitrary length of cylindrical samples [28]. According to these models, the maximum tensile stress σ occurs at the center of the sample and increases with B_0^2. The tensile strength σ_{max} of a damaged sample can be obtained from the applied magnetic field at which cracking was observed using the theoretical $\sigma(B)$ dependence predicted by the stress model. In this way, a value of $\sigma_{max} \sim 40$ MPa was estimated for the tensile strength of melt-textured YBCO [20], which is one order of magnitude lower than the tensile strength of low temperature superconductors. The reason is the presence of microcracks in bulk YBCO limiting the tensile strength of the material. The cracks begin to propagate when the external stress reaches the fracture toughness K_c of the material. In this case the tensile strength depends on K_c and on the initial size a of the largest crack according to the relation $K_c \propto \sigma a^{0.5}$. Typical values of the fracture toughness of melt-textured YBCO are in the range of $K_c \sim 2\,\mathrm{MPa\,m^{0.5}}$. The fracture toughness was found to increase by the incorporation of ductile particles impeding the propagation of the cracks. YBCO containing Ag particles shows an enhancement of K_c up to $2.4\,\mathrm{MPa\,m^{0.5}}$ compared with $K_c \sim 1.9\,\mathrm{MPa\,m^{0.5}}$ of samples without Ag inclusions [21]. We obtained very high trapped fields for YBCO disks with 10 wt% Ag, which were encapsulated in steel tubes. As shown in Fig. 7, a maximum trapped field of 11.4 T was measured at 17 K in a YBCO disk (diameter 26 mm, height 12 mm). In the gap between two of such YBCO disks a trapped field of 14.4 T was achieved before cracking of the samples was observed at lower temperatures.

3.4. Levitation forces

The levitation force between a permanent magnet and a superconductor cooled in the field of the magnet and containing a trapped magnetic flux can be written as $F \propto j_c R\, \mathrm{d}B/\mathrm{d}x$, where R is the size of the current loops in the superconductor and $\mathrm{d}B/\mathrm{d}x$ is the field gradient produced by the permanent magnet within the superconductor. As the superconductor approaches the permanent magnet after zero-field cooling the repulsive levitation force increases and reaches a maximum value for a small

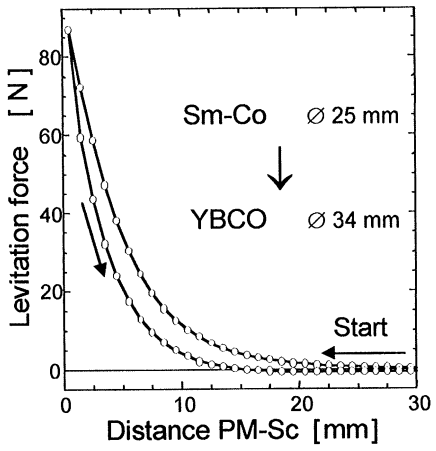

Fig. 8. Levitation force vs. distance between a Sm–Co (2:17) magnet and a YBCO disk after zero-field cooling.

distance. An example for the levitation force between a Sm–Co permanent magnet and a YBCO disk measured at 77 K is shown in Fig. 8. Maximum levitation forces up to $F \approx 90$ N were obtained in this case. The levitation force of this type of superconducting magnetic bearing is mainly limited by the surface field $B_s \sim 0.4$ T of the ferromagnetic permanent magnet which is lower than the maximum trapped field of YBCO at 77 K. Therefore, the bulk YBCO cannot be magnetized up to the maximum achievable trapped field. The maximum achievable levitation force for a given permanent magnet is that between the permanent magnet and its mirror image. The corresponding levitation pressure F/A with A as the area of the magnet is given by $F/A = B_s^2/(2\mu_0) = 25\,\mathrm{N/cm^2}$ for a permanent magnet with $B_s = 0.4$ T. The levitation pressure obtained in Fig. 8 achieves 72% of this upper limit. Much higher levitation pressures up to $2500\,\mathrm{N/cm^2}$ are expected if a superconducting permanent magnet with a trapped field as high as 11 T would be used instead of a conventional permanent magnet.

3.5. Magnetizing YBCO disks by pulsed fields

An important problem which has to be solved in order to realize YBCO magnets in superconducting bearings is to magnetize the superconductor. Pulsed magnetic fields can be used for magnetizing YBCO disks. However, large viscous forces act on the penetrating magnetic flux, especially in the case of short rising times. Therefore, (i) higher pulsed fields are needed and (ii) heat generation due to the rapid motion of magnetic flux strongly reduces the trapped field achievable at temperatures lower than 77 K [29]. We magnetized YBCO disks at 77 K by applying pulsed magnetic fields with different rise times and found that lower pulsed fields B_{ext} are required in order to trap a given field B_0 in the YBCO sample, if the rise time increases from 1 to 16 ms. For a rise time of 16 ms the same dependence of B_0 on B_{ext} was observed as for static external fields B_{ext} (after cooling the YBCO disk in zero magnetic field). No dependence on the size of the YBCO disks was observed. Therefore, we conclude that, at 77 K, no significant losses arise in the YBCO disks by applying pulsed fields with relatively long rise times of at least 16 ms.

4. Summary

The improvement of Nd–Fe–B and other rare-earth transition-metal permanent magnets is still in progress and their market is expanding. But no dramatic increase of their energy density $(BH)_{max}$ can be noted for the last decade or can be expected for the next future.

The trapped field of bulk melt-textured YBCO samples could be significantly enhanced in the temperature range between 55 and 80 K by doping the precursor powder with small amounts of Zn. The additional pinning observed in the Zn-doped YBCO can be explained by field-induced pinning defects developing around the Zn impurities which occupy Cu sites in the CuO_2 plane. The mechanical properties of the YBCO material were improved by the addition of Ag. The ductile Ag particles impede the propagation of microcracks under the influence of Lorentz forces, in particular those acting on the YBCO disks during magnetizing. Very high trapped fields up to 11.5 T on the top of a single YBCO disk and up to 14.4 T for a YBCO disk pair were achieved by the addition of silver and by using a steel bandage which produces a compressive stress on YBCO after cooling down from 300 K to the measuring temperature. Applications of the achieved high trapped fields require an effective procedure of magnetizing the bulk YBCO at temperatures below 77 K. Promising results were achieved by using pulsed magnetic fields with relatively long rise times of 16 ms.

Acknowledgements

The authors are grateful to O. Gutfleisch and A. Handstein for stimulating discussions. This work was supported by the German Bundesministerium für Bildung, Wissenschaft, Forschung und Technologie under contract # 13N6853. The support by Fonds der Chemischen Industrie is also gratefully acknowledged.

References

[1] K.H.J. Buschow, in: K.H.J. Buschow (Ed.), Handbook of Magnetic Materials, Vol. 10, North-Holland, Amsterdam, 1997, p. 463.

[2] J.R. Hull, Supercond. Sci. Technol. 13 (2000) R1.
[3] J.M.D. Coey, P.A.I. Smith, J. Magn. Magn. Mater. 200 (1999) 405.
[4] H. Samata, Y. Satoh, Y. Nagata, T. Uchida, M. Kai, M. der Lan, Jpn. J. Appl. Phys. 36 (1997) L476.
[5] J.J. Croat, J. Appl. Phys. 81 (1997) 4804.
[6] Y. Matsuura, IEEE Trans. Appl. Supercond. 10 (2000) 883.
[7] B. Grieb, IEEE Trans. MAG 33 (1997) 3904.
[8] A. Kirchner, D. Hinz, V. Panchanathan, K.-H. Müller, L. Schultz, IEEE Trans. MAG (2000), in press.
[9] H.A. Davies, C.L. Harland, J.I. Betancourt R., G. Mendoza S., Material Research Society Symposium Proceedings, Vol. 577, Mater. Res. Soc., Warrendale, 1999, p. 27.
[10] H.A. Leupold, A.S. Tilak, A. Potenziani II, J. Appl. Phys. 73 (1993) 6861.
[11] O. Gutfleisch, M. Kubis, A. Handstein, K.-H. Müller, L. Schultz, Material Research Society Symposium Proceedings, Vol. 577, Mater. Res. Soc., Warrendale, 1999, p. 3.
[12] O. Gutfleisch, M. Kubis, A. Handstein, K.-H. Müller, L. Schultz, Appl. Phys. Lett. 73 (1998) 3001.
[13] A. Handstein, M. Kubis, O. Gutfleisch, B. Gebel, K.-H. Gebel, J. Magn. Magn. Mater. 192 (1999) 73.
[14] C.H. Chen, M.S. Walmer, M.H. Walmer, S. Liu, G.E. Kuhl, G.K. Simon, Material Research Society Symposium Proceedings, Vol. 577, Mater. Res. Soc., Warrendale, 1999, p. 277.
[15] J.F. Liu, Y. Ding, Y. Zhang, D. Dimitar, F. Zhang, G.C. Hadjipanayis, J. Appl. Phys. 85 (1999) 5660.
[16] D.F. Lee, C.S. Partsinevelos, R.G. Presswood Jr., K. Salama, J. Appl. Phys. 76 (1994) 603.
[17] R. Weinstein, J. Liu, Y. Ren, R.P. Sawh, D. Parks, C. Foster, V. Obot, in: B. Batlogg, C.W. Chu, W.K. Chu, D.U . Gubser, K.A. Müller (Eds.), Proceedings of the 10th Anniversary HTS Workshop on Physics, Materials, and Applications, World Scientific, Singapore, 1996, p. 625.
[18] M. Morita, K. Nagashima, S. Takebayashi, M. Murakami, M. Sawamura, Mater. Sci. Eng. B 53 (1998) 159.
[19] G. Krabbes, G. Fuchs, P. Schätzle, S. Gruss, J.W. Park, F. Hardinghaus, G. Stöver, R. Hayn, S.-L. Drechsler, T. Fahr, Physica C 330 (2000) 181.
[20] Y.R. Ren, R. Weinstein, J. Liu, R.P. Sawh, C. Foster, Physica C 251 (1995) 15.
[21] P. Schätzle, G. Krabbes, S. Gruss, G. Fuchs, IEEE Trans. Appl. Supercond. 9 (1999) 2022.
[22] D. Lee, K. Salama, Jpn. J. Appl. Phys. Part 2, 29 (1990) L2017.
[23] P. Schätzle, W. Bieger, G. Krabbes, J. Klosowski, G. Fuchs, in: D. Dew-Hughes (Ed.), Applied Superconductivity 1995, Vol. 1, Institute of Physics Conference Series 148, IOP Publishing Ltd., Bristol, 1995, p. 155.
[24] G. Fuchs, P. Schätzle, G. Krabbes, S. Gruß, P. Verges, K.-H. Müller, J. Fink, L. Schultz, Appl. Phys. Lett. 76 (2000) 2107.
[25] M.R. Koblischka, A.J.J. van Dalen, T. Higuchi, S.I. Yoo, M. Murakami, Phys. Rev. B 58 (1998) 2863.
[26] S. Zagoulaev, P. Munod, J. Jegoudez, Phys. Rev. B 52 (1995) 10474.
[27] A.V. Mahajan, H. Alloul, G. Collin, J.F. Marucco, Europ. Phys. J. B 13 (2000) 457.
[28] T.H. Johansen, Phys. Rev. B 60 (1999) 9690.
[29] Y. Yanagi, Y. Itoh, M. Yoshikawa, T. Oka, A. Terasaki, H. Ikuta, U. Mizutani, in: K. Osamura, I. Hirabayashi (Eds.), Advances in Superconductivity, Vol. 2, Springer, Tokyo, 1998, p. 941.